Bull. Soc. R. Sci. Liège, 2024, **93**(1), 118–138 *Invited peer-reviewed paper*
doi:10.25518/0037-9565.12438

How does the Morphology of Jupiter's UV Main Auroral Emission Respond to Changing Conditions in the Magnetosphere?

Linus A. HEAD

Laboratory for Planetary and Atmospheric Physics, University of Liège
Correspondence to: LA.Head@uliege.be

Received: 24 May 2024 – Accepted 12 November 2024

Cet article a reçu un des Prix Annuels 2024 de la Société Royale des Sciences de Liège.
This paper was awarded one of the Annual Prizes 2024 of the Société Royale des Sciences de Liège.

Abstract

The ultraviolet aurorae of Jupiter, the brightest in the Solar System, are known to be of variable morphology. It is not entirely understood how this morphology varies with conditions present in Jupiter's extensive magnetosphere, such as its state of compression. This work presents the first use of automatic detection techniques to analyse the morphology of Jupiter's UV main auroral emission and link it with the state of the magnetosphere. A new reference oval for the average shape of the main emission is produced for the northern and southern hemisphere, based on images taken by Juno-UVS during its first 54 perijoves. A strong correlation is observed between the expansion/contraction of the main emission compared to these reference ovals in the northern and southern hemispheres, as well as between the main-emission expansion/contraction in the day and night hemispheres of the aurora, which indicates that the processes that work to vary the size of the main emission do so in a global way within the magnetosphere. The equatorward expansion also shows excellent correlation between with the equatorward latitudinal shift of the discrete aurora emission linked to Ganymede and the strength of the current in the magnetospheric current sheet, indicating that it is largely the stretching of the magnetic field of Jupiter that gives rise to the variable size of the main emission. Finally, compression of the magnetosphere is linked to a global main-emission contraction, one that occurs concurrently in both the north, south, day-side, and night-side hemispheres of the aurora, albeit to different extents. In all, these results indicate that the expansion or contraction of the UV main emission can be linked to a number of changes in the state of Jupiter's magnetosphere and magnetic field.

Keywords: Jupiter, aurora, magnetosphere

Résumé

Comment la morphologie de l'émission principale aurorale UV de Jupiter réagit-elle aux conditions changeantes dans la magnétosphère ? Les aurores ultraviolettes de Jupiter, les plus brillantes du système solaire, sont connues pour être de morphologie variable. On ne comprend pas entièrement comment cette morphologie varie en fonction des conditions présentes

dans la vaste magnétosphère de Jupiter, par exemple son état de compression. Ce travail présente la première utilisation de techniques de détection d'arc automatiques pour analyser la morphologie de l'émission principale aurorale UV de Jupiter et la relier à l'état de la magnétosphère. Un nouvel ovale de référence pour la forme moyenne de l'émission principale est produit pour l'hémisphère nord et sud, sur la base d'images prises par Juno-UVS au cours de ses 54 premiers périjoves. Une forte corrélation est observée entre l'expansion/contraction de l'émission principale par rapport à ces ovales de référence dans les hémisphères nord et sud, ainsi qu'entre l'expansion/contraction de l'émission principale dans les hémisphères diurnes et nocturnes de l'aurore, ce qui indique que les processus qui contribuent à faire varier la taille de l'émission principale le font de manière globale au sein de la magnétosphère. L'expansion équatoriale montre également une excellente corrélation avec le déplacement latitudinal vers l'équateur de l'empreinte de Ganymède et la force du courant dans la nappe de courant magnétosphérique, ce qui indique que c'est en grande partie l'étirement du champ magnétique de Jupiter qui donne naissance à la taille variable de l'émission principale. Enfin, la compression de la magnétosphère est liée à une contraction globale de l'émission principale, qui se produit simultanément dans les hémisphères nord, sud, côté jour et côté nuit des aurores, bien qu'à des degrés différents. Au total, ces résultats indiquent que la compression de la magnétosphère entraîne une contraction globale de l'émission principale.

Mots-clés : Jupiter, aurore, magnétosphère

1. Introduction

In 34 AD, Rome burned.

At least, that was the conclusion drawn by the Emperor Tiberius, who, seeing an ominous ochre glow over the port of Ostia, dispatched a Roman garrison to fight the flames. Instead, the port was found untouched, and the dull, red hue remained suspended in the western sky.

It is now suspected that this red glow was, in fact, the aurora borealis, pushed southwards to Italy from the Arctic Circle by unusually high solar activity. However, the Earth is not the only planet in our Solar System to possess aurorae; in fact, all the planets, to some extent, have their own equivalents to the Northern (and Southern) Lights. Venus, being bereft of a magnetic field, does not concentrate its aurorae to the northern and southern magnetic poles, but rather experiences a diffuse auroral emission over the entire sunward hemisphere (the "dayglow") as charged particles from the Sun impact the atmosphere (Gérard et al., 2008). Mars, also lacking a strong global magnetic field, nevertheless has small "patchy" aurorae that occur over regions of its crust that still maintain a residual magnetic field (Soret et al., 2021). However, the brightest, largest, and most interesting aurorae are those of Jupiter. As befitting the King of the Solar System, the auroral crown of Jupiter encompasses a region of width more than three times the diameter of the Earth. Jupiter's aurorae, in the far ultraviolet waveband (120 nm to 170 nm) alone, emit 100 times as much power as Earth's aurorae (Clarke et al., 2004) and more energy per second than is consumed by all of humanity (Potter, 2021). However, Jupiter's aurorae are not simply bright, brutish emitters of light; they also show hitherto-unexplained complexity and

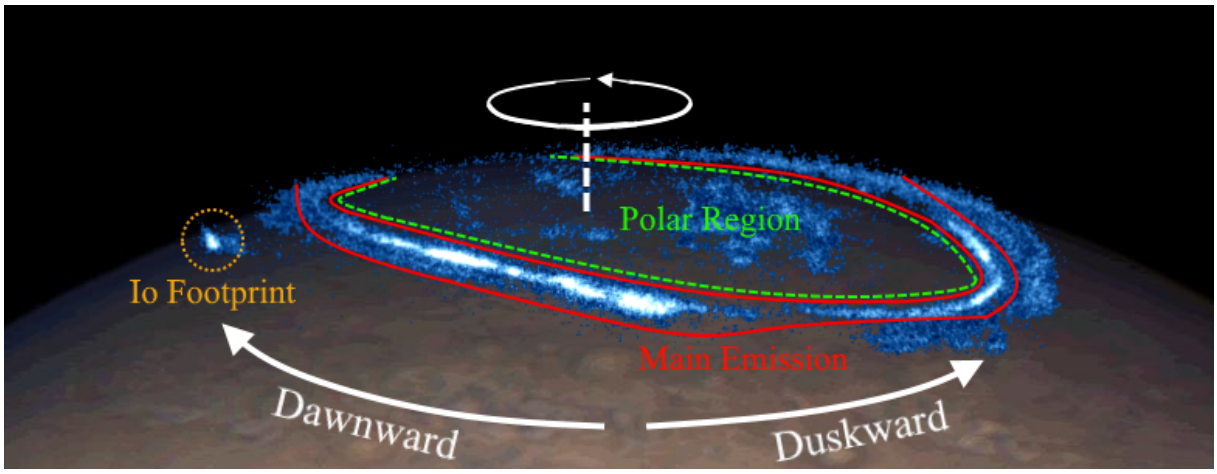

Figure 1: An example view of Jupiter's northern UV aurora superimposed onto a visible-light image of Jupiter, with typical region divisions annotated. The main emission is denoted by the region contained within the two red solid lines, and the polar emission by the region enclosed by the green dashed line. The equatorward emission comprises all auroral emission not found in these two regions. The position of the Io footprint has been indicated by an orange dotted circle. The sense of rotation as well as the definitions of "dawnward" and "duskward" have been annotated.

variability, including characteristics that are entirely absent from the aurorae of the Earth.

The ultraviolet aurorae of Jupiter are typically separated into three regions, shown in Fig. 1. Firstly, there is the conspicuous "main auroral emission" (ME), always present in images of the Jovian aurora. It presents itself as a bright, roughly continuous circumpolar band of auroral emission (the region denoted by solid red lines in Fig. 1), though both the brightness and continuity of the ME is variable. The ME will appear the most familiar to those acquainted with the Earth's aurorae, which take the form of similar "loops" of auroral emission around the magnetic poles of the Earth. However, the similarity between these two aurorae are merely superficial, and the physical processes responsible for their generation differ considerably. Secondly, there is the "polar emission," which describes the auroral emission poleward of or internal to the ME. This bears resemblance to the polar-cap emission sometimes seen in Earth's aurora (Delamere et al., 2024) though, once again, this is simply a surface-level similarity. Finally, the "outer emission" describes the auroral emission equatorward of or external to the ME, which typically takes the form of a diffuse auroral emission punctuated by bright, transient, amorphous aurorae, linked to injections of plasma in Jupiter's magnetosphere (Dumont et al., 2018). Also sometimes included with the outer emission are the auroral moon footprints – discrete spots of auroral emission that are magnetically linked to (at least) three of Jupiter's four Galilean moons – though the unique origin of these features typically merit their own separate category. While all parts of the Jovian aurora are interesting and deserve in-depth discussion, this article will concentrate almost entirely on the ME.

Whereas the polar and outer emission can both dramatically change in visibility, the ultraviolet ME is an ever-present feature of the Jovian aurora. However, although the ME is always present, it can nevertheless show a great deal of variability. Jupiter's aurora rotate with the planet; the "shape" of the ME remains fixed on the globe of Jupiter. This stands in contrast to the aurorae of the Earth, which have shapes that remain fixed with respect to the position of the Sun (Feldstein, 1986). However, though the general shape of the aurorae rotates with Jupiter, its characteristics, such as brightness, can depend on local time with respect to the Sun. The mere fact that the appearance and brightness of the main emission varies systematically with local time betrays something rather surprising about the aurorae of the Jupiter. Jupiter is surrounded by its extensive magnetosphere, which is a region of plasma surrounding the planet that is held in place by Jupiter's magnetic field rather than by Jupiter's gravity. The size of this magnetosphere (that is, the distance between Jupiter and the magnetopause on the side facing the Sun) varies between 45 and 100 Jupiter radii (Khurana et al., 2004); compare this to Earth's own magnetosphere, which is only 10 times wider than Earth. This difference is due to two main factors. Firstly, Jupiter's intrinsic magnetic field is 20 000 stronger than Earth's. Secondly, the plasma of Earth's magnetosphere is made primarily of hydrogen, whereas Jupiter's magnetosphere consists overwhelmingly of sulphur and oxygen ions from its volcanic moon, Io, which is the source of some $1000\,\mathrm{kg\,s^{-1}}$ of magnetospheric plasma (Saur et al., 2004). This means that Jupiter's magnetosphere contains an internal source of heavy plasma, which inflates the magnetosphere from the inside. Unlike for the Earth, where aurorae arise mainly from the interaction between the magnetosphere and the solar wind, Jupiter's large and energetic magnetosphere contains many processes that give rise to auroral emission, without the need for the energisation of magnetospheric plasma by the solar wind. These processes are connected to the aurora along magnetic field lines; hence, we speak of a magnetic mapping between the a particular auroral emission and its source region in the magnetosphere, with more distant magnetospheric sources mapping to auroral emission that is closer to Jupiter's magnetic poles. The aurora is therefore a "mirror" for processes occurring in the magnetosphere. It was long thought that those processes taking place deep within Jupiter's magnetosphere – such the process(es) that give rise to the ME (Cowley and Bunce, 2001; Saur, 2004), in the middle magnetosphere between 20 and $60\,R_\mathrm{J}$ (Vogt et al., 2011) – would be almost entirely insulated from the influence of the solar wind (Khurana, 2001). However, the observation of a marked local-time dependence of the morphology and brightness of the ME indicates that the solar wind can indeed have an effect on the middle magnetosphere. For example, the brightest segment of the ME is typically the dusk-side segment (Bonfond et al., 2015; Groulard et al., 2024), which can be seen in Fig. 2. It can also be seen that the morphology of the ME, and not simply its brightness, is dependent on local time. We can see that the dusk-side ME is typically wider and more irregular than the dawn-side ME, which tends to present as a thin, neat band of auroral emission (Nichols et al., 2009; Palmaerts et al., 2023), though the general shape of the ME as a whole remains essentially fixed on the globe of Jupiter. This dusk-side disruption is more easily visible in Fig. 2a due to Juno's lower altitude and hence greater spatial resolution, allowing for the resolution of smaller auroral features. However, while Jupiter's ME is essentially fixed to the globe of Jupiter, its shape can vary slightly with local time; the ME has previously been observed to contract slightly at dusk

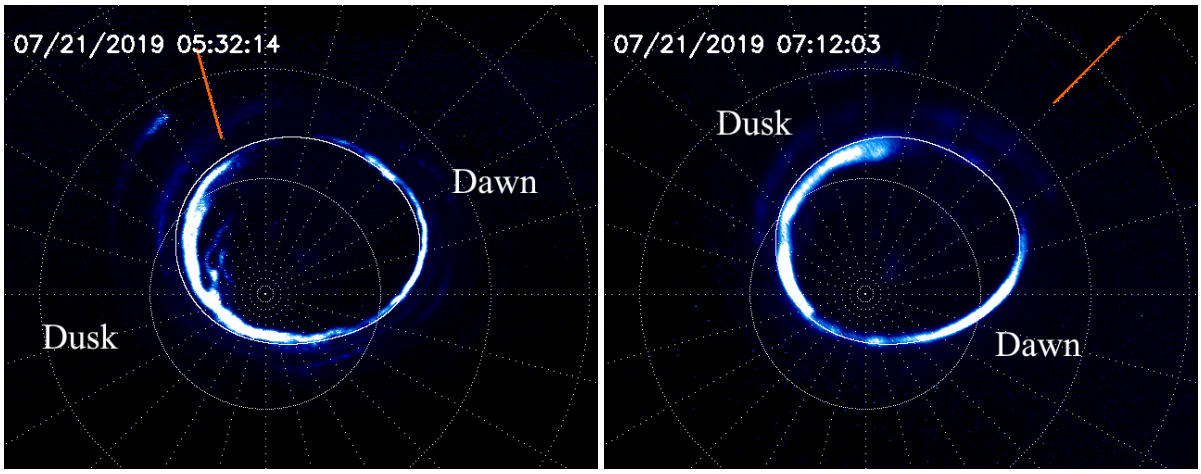

Figure 2: Two UVS images of the southern aurora, composed of 100 Juno spins, taken from perijove 21. The time of the central spin is annotated in both cases. A 15°-by-15° grid in System-III longitude and planetocentric latitude is overlain on the aurora. The solid white line gives the location of the average shape of the ME. The angle of the Sun (sub-solar longitude) has been annotated as a solid orange line.

and expand slightly at dawn (Grodent et al., 2003). However, this conclusion was drawn from images taken exclusively by the Hubble Space Telescope (HST), in orbit around the Earth and hence only capable of viewing the day-side hemisphere of Jupiter and hence only a portion of the aurora. To understand the full local-time variability of the ME, we require images of both hemispheres of the aurora.

It is important to distinguish these two forms of variability in the morphology of the ME:

1. The *local* shape of the ME is dependent on local time; as Jupiter rotates, the part of the ME in the dawn-side hemisphere will gently expand outwards and the part in the dusk-side hemisphere contract gently inwards. This would be the case even if the state of the state of the magnetosphere remained static.

2. The *global* size of the ME is hypothesised to be dependent on the state of the magnetosphere; in addition to the above dawn (dusk) expansion (contraction) of the ME, the entire ME may undergo changes in size in response to compression of the magnetosphere by the solar wind or inflation of the magnetosphere by increased mass outflow from Io. This latter variability in size is the focus of this work.

Presently, it is not fully understood how the global size of the ME varies, nor how it responds to the state of the magnetosphere, as the latter is best investigated via in-situ measurements made by spacecraft. For example, during periods of increased mass outflow from Io – which may be related to increased volcanic activity, though this link is disputed by, e.g., Roth et al. (2020) – the ME was observed to expand equatorwards (Bonfond et al., 2012); see Fig. 3b. This is due to the increased plasma density in the equatorial current sheet, which works to stretch the

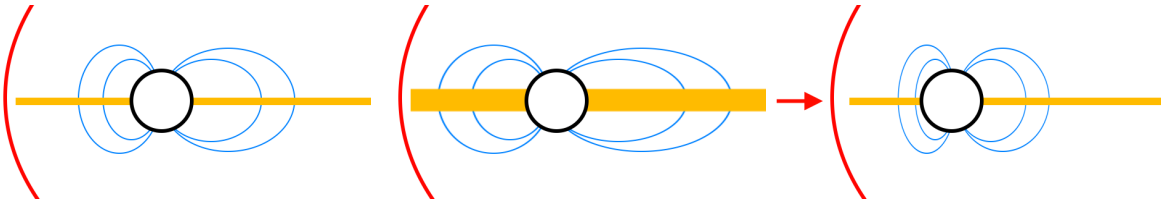

(a) Original state

(b) 1: Stretching by mass outflow from Io

(c) 2: Compression by the solar wind

Figure 3: Schematic view of the two sources of magnetospheric variability described in this work. The blue solid lines show a set of arbitrary magnetic fields. The magnetopause position is given by a solid red line. The equatorial plasma sheet is denoted by the yellow rectangle.

magnetic field lines outwards. The source region of the ME (at a distance of around $20 R_J$ for both corotation breakdown and plasma turbulence) would therefore connect to a more interior magnetic field line, which itself connects to the ionosphere at a lower latitude, moving the ME equatorwards. Additionally, models show that compression of the magnetosphere by the solar wind should lead to a contraction of the ME, at least on the day side (Chané et al., 2017); see Fig. 3c. Observational, solar-wind compression of the magnetosphere has been linked to particular auroral morphologies (Yao et al., 2022), though this work did not go as far as to investigate the response of the size of the ME.

Whatever its original source (inflation of the magnetosphere by Io mass outflow, compression of the magnetosphere by the solar wind, or indeed both), two intermediate processes can influence the observed size of the ME: a variable magnetic field or a mobile ME source in the magnetosphere; this is explained diagrammatically in Fig. 4. Both of these intermediate processes could cause expansion or contraction of the ME and would be difficult to distinguish. However, Jupiter possesses an excellent reference point to help disentangle this degeneracy: its moons. As mentioned previously, the innermost three Galilean moons (Io, Europa, Ganymede) have all been observed to have footprints in Jupiter's aurora, connected with the position of the moon itself along a magnetic field line. Whilst the source region of the ME may be of variable magnetospheric depth, Jupiter's moons certainly are not. Therefore, if the footprint of Ganymede, as the moon closest to the ME source region, is observed to move at the same time as the ME, then the magnetic field is stretching, whereas if the footprint of Ganymede remains stationary when the ME moves, then the ME source region is likely moving (Vogt et al., 2022b). Of course, these two intermediate processes are not mutually exclusive, but this type of analysis will at least allow us to determine whether one process dominates over the other. Previous analysis of this type found that the footprint of Ganymede sometimes, but not always, moves with the ME (Vogt et al., 2022b). However, this work used image data from the Hubble Space Telescope, which, as a telescope in orbit around the Earth, has considerable bias in viewing angle. Additionally, the imaging instrument used (HST-STIS) has large uncertainties in its pointing, which translates to large uncertainties in the observed position of the ME on the globe of Jupiter and hence also in its expansion. Use of images from the UltraViolet Spectrograph (UVS) in-

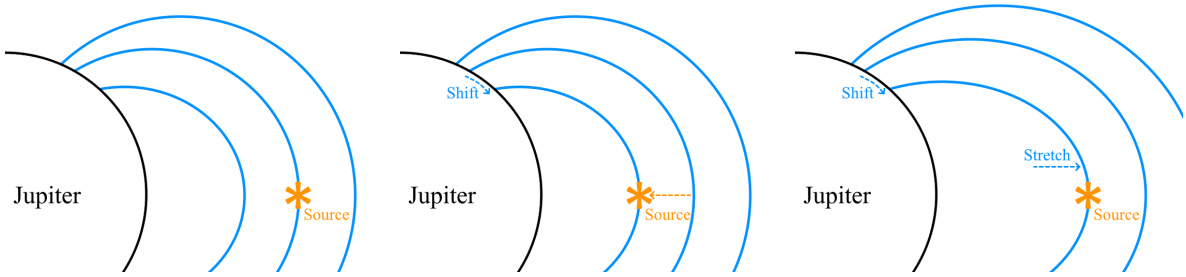

(a) Original state (b) 1: Source region moves (c) 2: Magnetic field stretches

Figure 4: Schematic view of the two ME expansion scenarios described in this work. The blue solid lines show a set of arbitrary magnetic fields. The magnetospheric source region (either Ganymede or the ME source region) is given by an orange star. In both scenarios, an identical shift in auroral latitude on the globe of Jupiter is produced.

strument on board Juno, which have almost perfect pointing and no bias in viewing angle or coverage of the aurora, would allow us to achieve greater clarity regarding the process(es) that cause the ME to vary in size.

With all this in mind, the aim of this work is to use novel image-analysis techniques on Juno-UVS images of the northern and southern UV aurora of Jupiter to examine how the expansion of the ME varies and to link this to conditions in Jupiter's magnetosphere.

2. Methods

The "basic" image type used in this work is a 1024×1024-pixel polar projection of the northern and the southern aurora. The UVS instrument on board Juno does not capture an instantaneous image of the entire aurora. Instead, the spacecraft scans a small region of the aurora with each of its 30-second rotations; 100 consecutive spins are collated and projected to the ellipsoid of Jupiter to provide a series of "complete" images of the aurora, as would be viewed from above the northern pole of Jupiter; an example is given in Fig. 5a. Within one of Juno's passes close to Jupiter (a "perijove" or "PJ"; approximately once every 14 days), UVS will capture roughly 1000 spins ($\sim$ 8 hours) of images of the aurora. For each of Juno's first 54 perijoves, two of these 100-spin-collated images, one of the northern aurora and one of the southern aurora, were selected as the "master" images for that perijove. In total, 106 images were used in this work, 53 of the aurora in each hemisphere; during PJ2, Juno had to enter safe mode and no image data were collected.

For this work, it was decided to perform (semi-)automatic detection of the location of the ME in each of the master images. The advantages of this over manual designation of the ME location are essentially two-fold: firstly, to allow for more objective and consistent positioning of the ME in the image; and secondly, to permit the quick and efficient processing of large numbers of images. To detect the ME, a structure composed principally of one or more auroral arcs, a new arc-detection process was developed, centred around the convolution of the image

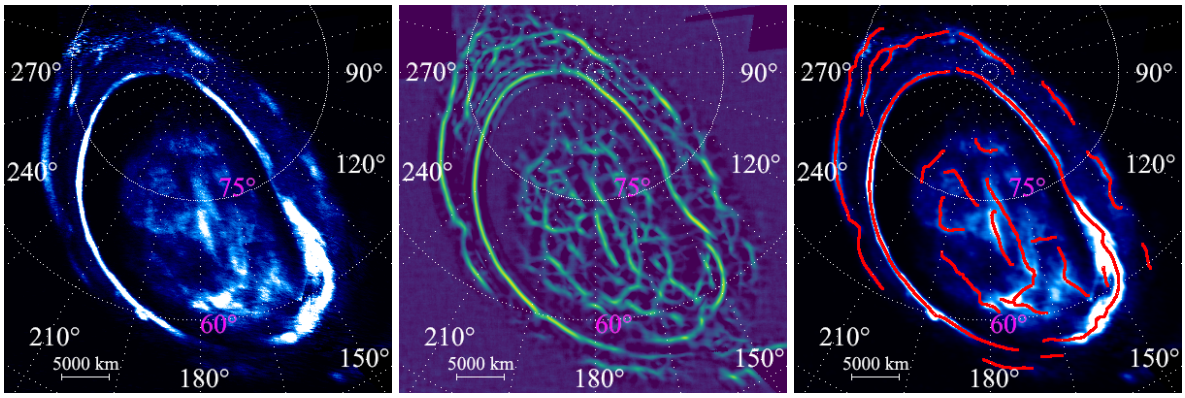

(a) UVS master image (b) Convolved image (c) Detected auroral arcs

Figure 5: The arc-detection algorithm applied to the UVS master image of the northern aurora from perijove 6. A 15°-by-15° grid in System-III longitude and planetocentric latitude is overlain on the aurora. The System-III longitude of certain gridlines are given in white, and the planetocentric latitudes of certain gridlines in magenta.

with a model arc profile. By convolving the base auroral image with this model arc profile (at a number of different rotations), the "arcness" (between 0 and 1) of each pixel of the original image can be calculated. It can be seen in Fig. 5b that this method successfully highlights the arcs present in the original image. From this, the positions of individual arcs can be easily extracted, as in Fig. 5.

Once the arcs have been detected in each master image, the final step is to extract those that form part of the main emission. However, this is not a straightforward task for an automated algorithm; the main emission shows great variability in its size and morphology, and is frequently close to or overlaps other arc-like structures in the aurora that an automatic extraction algorithm would likely mis-extract. Therefore, the designation of the ME was performed semi-manually for each image, to ensure that the entire ME, and only the ME, was corrected extracted in each case. The region roughly containing the ME was manually defined for each image; any automatically detected arcs that pass through this manually defined region were considered to form part of the ME. In this way, the position of the ME was extracted in each of the master images, ready for analysis.

3. Results and Discussion

3.1. A new reference oval for the ME

The main aim of this work is to analyse the variability in the expansion of the ME; as such, it is necessary to define a "reference contour" that designates the zero-expansion position of the ME. In this work, the average positions of the ME in the north and the south over the first 54 perijoves was taken as the reference ME contour. This was performed by stacking the polar-projected master images (separately for the north and south) then taking the pixel-wise median

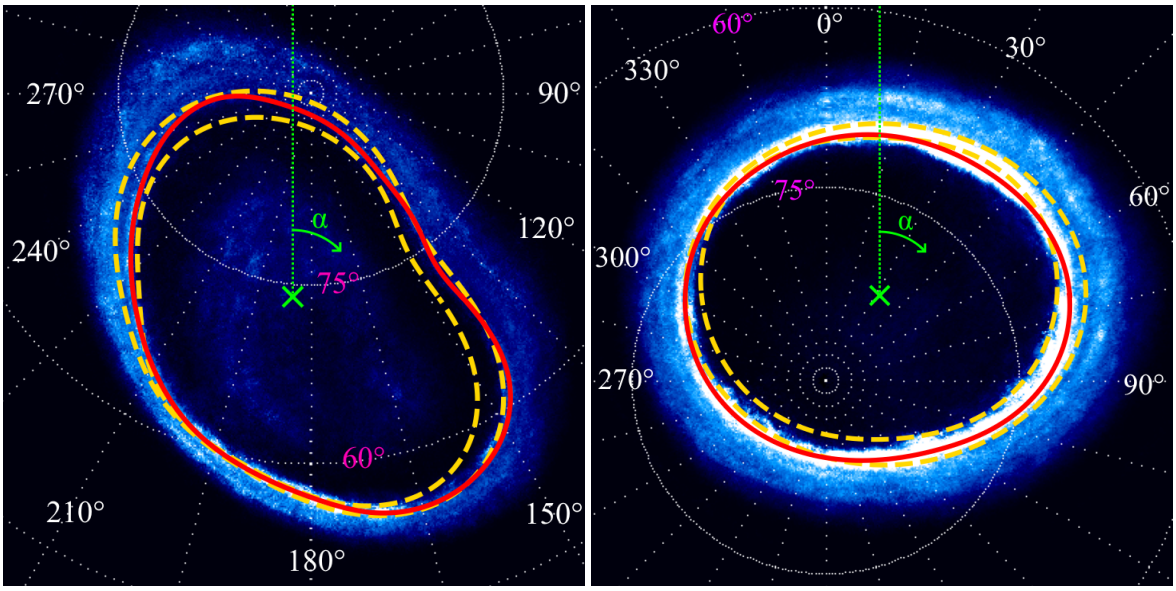

(a) North (b) South

Figure 6: The ME reference ovals defined in this work, overlain on the average ME for each hemisphere. The new UVS reference oval is shown as a solid red line. The expanded and contracted HST ME reference ovals from Bonfond et al. (2012), shown as dashed yellow lines, are included for comparison. The pseudo-magnetic-coordinate reference point is denoted by a green cross, alongside the sense of pseudo-magnetic angle α. A 15°-by-15° grid in System-III longitude and planetocentric latitude is overlain on the aurora. The System-III longitude of certain gridlines are given in white, and the planetocentric latitudes of certain gridlines in magenta.

of this stack. This produces a median-average image of the aurora for both hemispheres, as shown in Fig. 6. Median averaging reduces the impact of noise in the data, and so the transient and variable emission of the polar region is masked, but the more-constant and brighter emission of the ME remains prominent. The arc-detection algorithm was applied to this median image (as described above in Sect. 2) and the position of the ME extracted to provide a reference contour for the ME in both the northern and southern hemispheres, against which the position of the ME in any given image can be compared to calculate its relative expansion.

3.2. The global nature of ME expansion

The relative expansion of the ME in the master images from each perijove can be compared between hemispheres, to investigate whether the processes that occur to vary the size of the ME have timescales shorter or longer than the time required for Juno to pass from one hemisphere to another (around 4 hours). Figure 7 shows an excellent linear correlation ($R^2 = 0.74$) between the expansion of the northern ME and the expansion of the southern ME. Additionally, the fitted linear relation passes through the origin (to within the uncertainty in the data), which supports

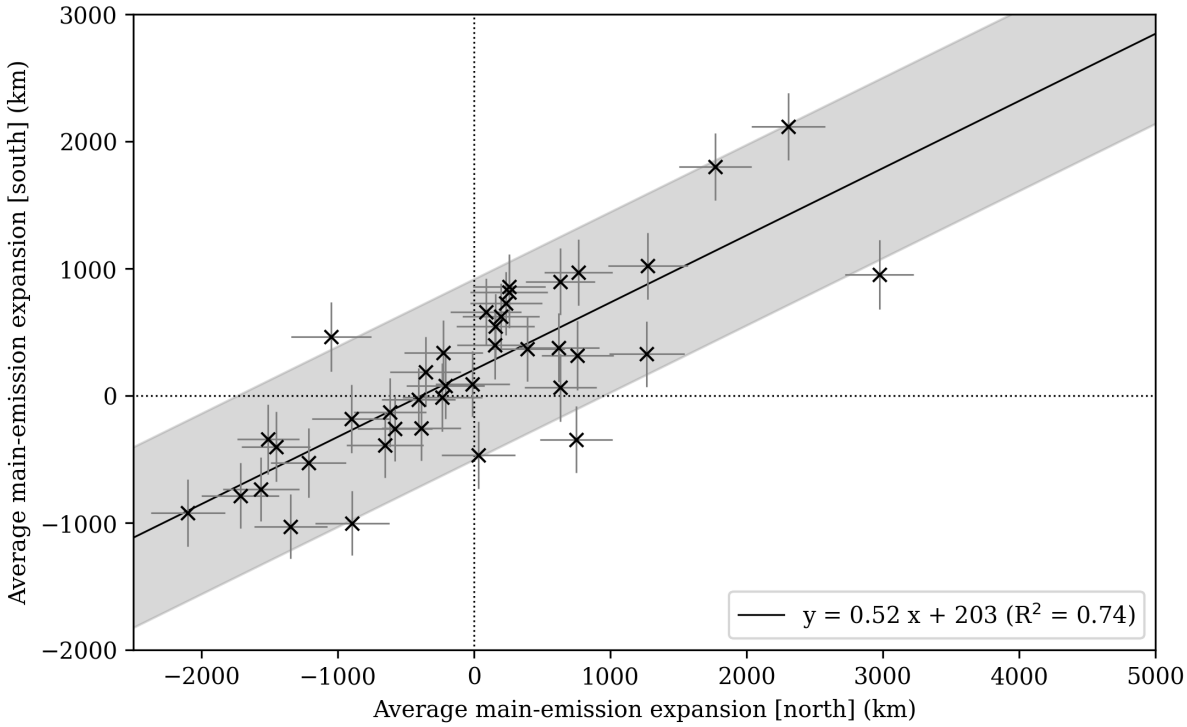

Figure 7: The median-averaged global ME expansion from the UVS reference oval in the north vs. in the south for perijoves 1 through 54. Perijoves with sufficiently poor coverage in the northern hemisphere such that the position of no part of the ME can be reliably determined are omitted. The uncertainty in the global ME expansion has been estimated from the HWHM of the Gaussian profile arc-detector convolution element (3 px), which correlates with the width of the ME arcs in the convolved image. The fitted relationship is given by a solid black line; its form and R-squared goodness-of-fit value are given in the legend. The 1σ confidence level of the fit is given by the shaded region. The position of the origin is denoted by two dotted black lines. Negative values of ME expansion indicate a global contraction of the ME.

the use of the defined reference ovals as the "average" position of the ME. The fact that the expansions of the northern and southern ME show such excellent correlation indicates that the process(es) responsible for them vary over timescales longer than the ~ 4 hours required for Juno to pass between hemispheres during a perijove; it can thus be said that these processes affect the northern and southern hemispheres simultaneously. This result provides the first hint toward the global nature of these processes within Jupiter's magnetosphere, rather than being confined to particular magnetospheric sectors.

In addition to a comparison between hemispheres, the expansion of the ME can be explored separately in the day-side and night-side half of the aurora. Figure 8 shows excellent correlations($R^2 = 0.91$ for the north, 0.73 for the south) between the mean ME expansion on the day and night halves of the aurora, in both the northern and southern hemispheres. Here again, the linear relationships between the day- and night-side ME expansions pass though the origin, within the uncertainty of the data. This result indicates that the day- and night-side ME expand together; when the day-side ME is expanded or contracted from its average position, so too is the night-side ME. This indicates that whatever process(es) are responsible for varying the expansion of the ME occur simultaneously in both the day-side and night-side magnetosphere. Combined with the previous result – that the northern and southern ME also vary together – this strengthens the idea that it is a global magnetospheric process that is responsible for the variable expansion of the ME.

3.3. Distinguishing between the sources of variable ME expansion

Whatever the global magnetosphere process is that gives rise to the variable size of the ME, it must be somehow transmitted from the magnetosphere to the aurora, perhaps via a displacement of the ME source region or the topology of the magnetic field. Features in the Jovian aurorae are known to magnetically map to processes occurring in the magnetosphere. The ME is no exception, and is thought to map to a region of the middle magnetosphere at a distance of around $30\,R_\mathrm{J}$. Two scenarios are envisaged that could explain the observed expansion and contraction of the ME (Vogt et al., 2022b):

- The distance into the magnetosphere at which occur the processes that give rise to ME may be variable (Fig. 4b). If the ME source region moved outwards in the magnetosphere, it would be connected to a more distant magnetic field line which would map to a more poleward position in the ionosphere; the ME would be observed to contract.

- The magnetic field of Jupiter may itself undergo stretching or compression (Fig. 4c). In this scenario, a stationary ME source region would map to a more equatorward location in the ionosphere if the magnetic field underwent an outward stretch, perhaps under the influence of increased mass outflow from Io (Promfu et al., 2022); the ME would also be observed to expand.

Indeed, these two scenarios are not mutually exclusive and may both influence the expansion of the ME to some extent. Determining which of these processes is dominant would be difficult

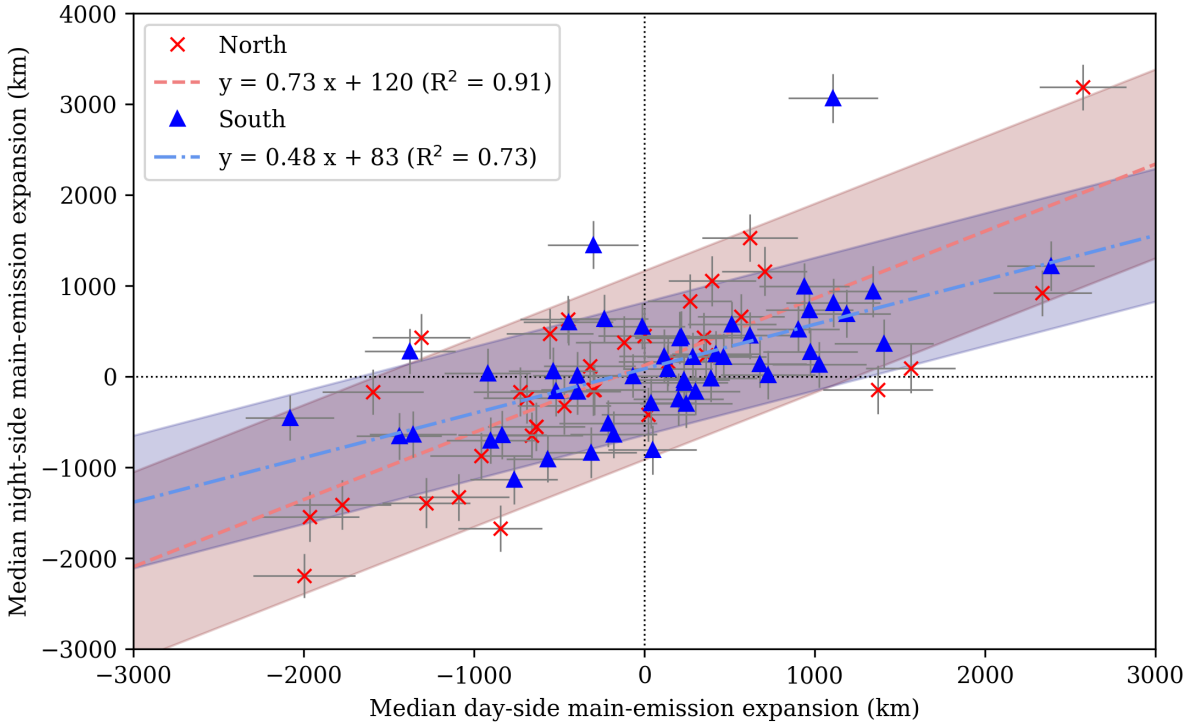

Figure 8: The median-averaged global ME expansion from the UVS reference oval in the day-side hemisphere vs. in the night-side hemisphere for perijoves 1 through 54, for the northern (red crosses) and southern (blue triangles) aurorae. Perijoves with excessively poor coverage in the northern hemisphere are omitted. The uncertainty in the global ME expansion has been estimated from the half-width half-maximum value of the Gaussian profile arc-detector convolution element (3 px), which correlates with the width of the ME arcs in the convolved image. The fitted relationships are given by a red dashed line and a blue dot-dashed line for the northern and southern hemisphere respectively; their forms and R-squared goodness-of-fit values are given in the legend. The 1σ confidence levels of the fits are given by the red and blue shaded regions, for the northern and southern hemispheres respectively. The position of the origin is denoted by two dotted black lines. Negative values of ME expansion indicate a global contraction of the ME.

based on the expansion of the ME alone, due to the degeneracy in the effect on ME expansion that these two scenarios would incur and the challenges involved in observing the position of the ME source region directly. However, there are auroral features of which the magnetospheric source region is known to be fixed in distance from Jupiter, most notably the moon footprints. By observing whether the footprint of Ganymede (as the moon closest ($15\,R_J$) to the assumed ME source region at $30\,R_J$ with an easily visible auroral footprint) shifts in magnetic latitude in conjunction with the expansion of the ME, these two proposed scenarios can be differentiated. If the Ganymede footprint (GFP) moves with the ME, it is likely that a stretched magnetic field is predominantly responsible for the expansion of the ME. However, if the GFP is not observed to move with the ME, it is more likely that the ME source region is moving to (largely) produce the observed expansion of the ME. In both of these scenarios, the latitudinal shift of the Io footprint (IFP) is unlikely to respond to the expansion of the ME, since stretching of the magnetic field lines would occur more strongly at greater distances from Jupiter. This is because, in addition to Jupiter's internally generated magnetic field, there exists also a contribution to the global magnetic field by Jupiter's equatorial plasma sheet (or magnetodisc), a plasma overdensity that occurs at the equator within Jupiter's magnetosphere external to the orbit of Io, due to the outward transportation of mass from the Io plasma torus (Connerney et al., 2020). This stretching in the magnetic field would be likely due to a variable contribution of this equatorial-plasma-sheet (external) magnetic field to the global magnetic field. A stronger external magnetic field would stretch the field lines outward, which may occur during periods of increased mass outflow from Io (Nichols, 2011; Bonfond et al., 2013).

Figure 9a shows a reasonable linear relationship ($R^2 = 0.42$) between the expansion of the ME and the latitudinal shift of the GFP; in other words, the GFP, for the most part, moves with the expansion of the ME, and therefore it is likely that a stretching in the magnetic field can account for a large proportion of the observed range of expansion of the ME. Though the R^2 value of 0.42 does not allow for the drawing of robust conclusions based on the behaviour of the GFP alone, it must be interpreted in the context of the complete lack of correlation ($R^2 = 0.00$) between the expansion of the ME and the latitudinal shift of the IFP, which is perfectly in line with the scenario presented above. This conclusion is supported by the results of recent work (Vogt et al., 2022b), though the result presented here is both stronger and applicable to the full ME, rather than only the day-side sector. The gradient of the linear relation between the expansion of the ME and the GFP (~ 0.5) is also in line with theoretical predictions; the ME source region at around $30\,R_J$ is twice as far from Jupiter as Ganymede ($15\,R_J$) and so it is expected that the ME move twice as much (in absolute km terms) than the GFP for a given stretch in the magnetic field.

This influence of the magnetodisc magnetic field can also be more directly investigated using in-situ measurements from Juno. The strength of this external magnetic field, parameterised in terms of the magnetodisc current constant, has been calculated from Juno measurements for the first 32 perijoves (Vogt et al., 2022a). As seen in Fig. 9b, the expansion of the both the ME and the GFP shows a reasonable linear dependence on the magnetodisc current constant, though again it must be emphasised that, when drawing conclusions, results should be interpreted together rather than putting too much emphasis on individual R^2 values. Here again, this

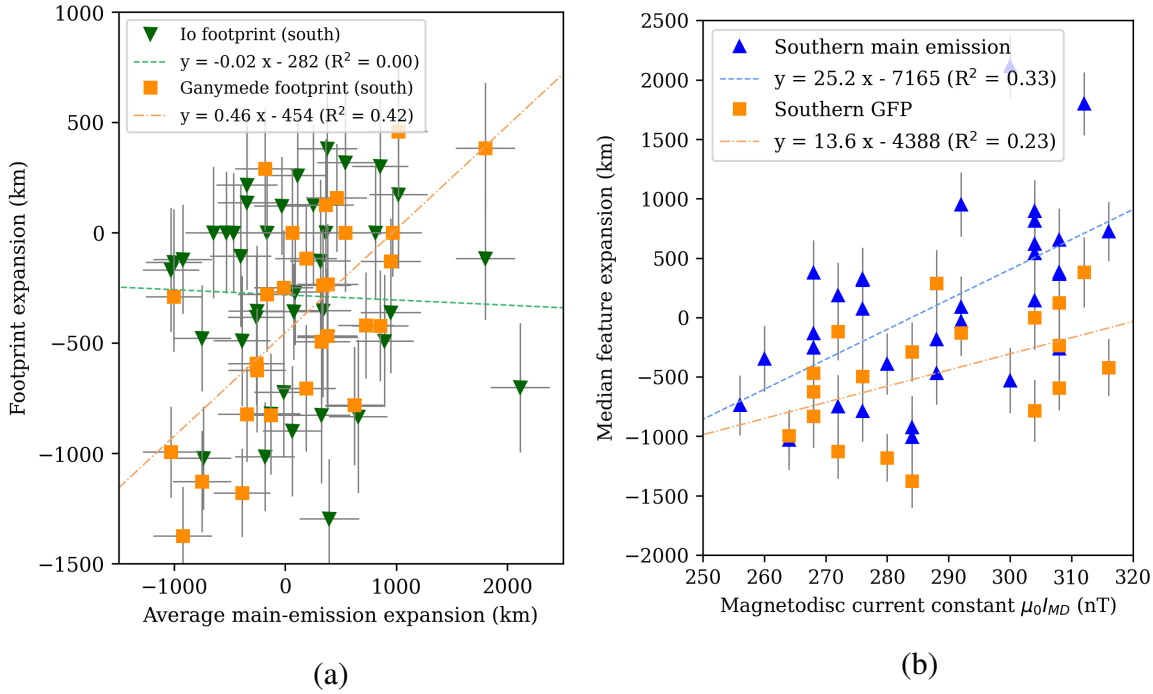

Figure 9: (a) The median-averaged expansion of the southern ME relative to the UVS reference oval vs. the expansion of the Io and Ganymede auroral footprints relative to their magnetically mapped contours at 900 km. The expansion of the Io footprint is denoted by green triangles, and that of the Ganymede footprint by orange squares. (b) The magnetodisc current constant fitted to perijoves 1 through 20 after Connerney et al. (2020) vs. the median-averaged global expansion of the ME relative to the UVS reference oval and the expansion of the Ganymede auroral footprint relative to its mapped contour at 900 km, in the southern hemisphere. The global ME expansion in the south is denoted by blue triangles, and the expansion of the southern Ganymede footprint by orange squares.

relationship is stronger for the ME, as expected given its more-distant source region. This relationship between magnetodisc current constant and ME expansion was not found in previous analysis of HST data (Vogt et al., 2022b), likely due to large uncertainties in the position of the limb of Jupiter in HST images (Bonfond et al., 2017). Of course, variations in the density of the magnetodisc is not the only possible source of stretching in the magnetic field, which likely explains some proportion of the scatter in the points in Fig. 9b. The variable pressure of the solar wind also works to compress the magnetosphere (and hence the magnetic field) to variable extents. To distinguish between the relative effect of internal sources (mass outflow from Io) and external sources (solar wind) of magnetic stretching, information on the timescales of the expansion of the ME is required, since magnetic stretching by the solar wind is predicted to occur over shorter timescales (Chané et al., 2017) than those induced by the mass outflow from Io (Bagenal and Delamere, 2011; Nichols et al., 2017; Tao et al., 2018). For the time being, these two independent measures indicate that the ME varies its size due to a variable stretching of the magnetic field in the middle magnetosphere.

3.4. Comparison with the compression of the magnetosphere

The Juno spacecraft performs a very elliptic orbit around Jupiter that, when the apojove is not aligned down Jupiter's long magnetotail, takes it out of the magnetosphere before plunging back in. By measuring the altitude at which Juno crosses into the magnetosphere (via the detection of characteristic low-frequency radio emission trapped in Jupiter's magnetopause), it is possible to determine the state of compression of the magnetosphere (Yao et al., 2022). This traversal of the magnetopause necessarily occurs when Juno is far from Jupiter, and hence there are no Juno-UVS images of the aurora that coincide with magnetopause crossings. However, contemporaneous HST images of the aurora are available in many cases, which allow for the direct investigation of the expansion of the ME under conditions of known magnetospheric compression, though these images are necessarily only of the day-side aurora visible from Earth.

Figure 10 shows that, for the northern aurora (the southern aurora is less visible from Earth and hence ignored in this section), the cases where the magnetosphere is known to have been compressed typically show a ME that is more contracted compared to the cases where the magnetosphere is known to have been uncompressed. Note that images taken with HST tend to show global contractions. This is due to a number of factors: the comparative neatness of the dawn-side ME; the result (as above) that the dawn-side ME tends to be contracted; the inability of HST to view the night-side ME. In all, this means that the contraction of the dawn-side ME tends to dominate the global size of the ME as seen by HST. Therefore, care must be taken when comparing HST ME sizes with those seen by Juno-UVS, though it is entirely possible to compare HST images among themselves. The 1σ ranges for the compressed and uncompressed cases overlay only very slightly, indicating that this difference in typical contractions of the ME is likely statistically significant at this level. This indicates that a compressed magnetosphere leads to a contracted ME, at least on the day side. However, it has previously been shown that the whole ME contracts and expands in unison, and so it can be said that compression of the magnetosphere works to compress Jupiter's magnetic field and hence contract the entire ME.

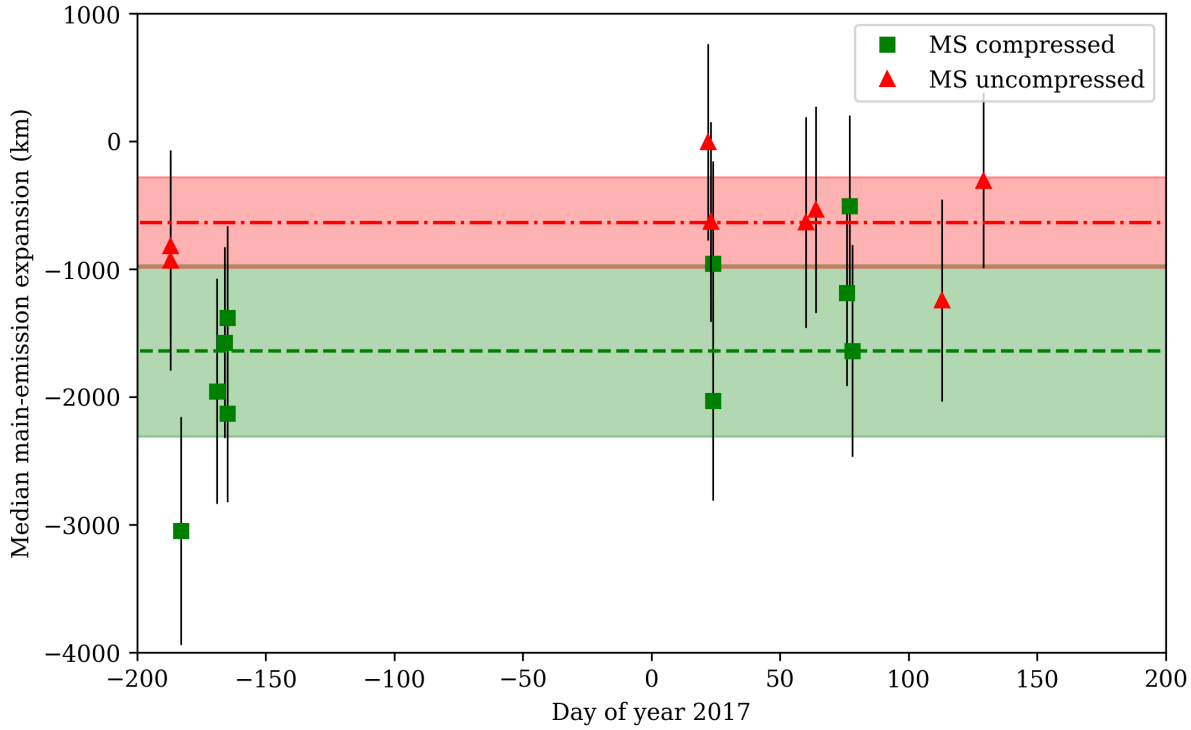

Figure 10: The imaging date (as day-of-year 2017) vs. the median-averaged global ME expansion from the UVS reference oval for those northern-hemisphere HST image series with known magnetospheric compression states, after Yao et al. (2022). An uncompressed magnetosphere is denoted by a red triangle and a compressed magnetosphere by a green square. The average ME expansion in the uncompressed-magnetosphere case (−600 km) is denoted by a red dot-dashed line, and that in the compressed-magnetosphere case (−1600 km) by a green dashed line. The shaded regions around each average-value line denote the 1σ range.

4. Conclusion

In this work, novel image-analysis techniques have been employed to investigate how the size of the ME responds to changing conditions in the magnetosphere. The following results are presented in this work:

- The global level of expansion/contraction of the ME is excellently correlated between the northern and southern ME; the northern and southern ME expands and contracts in unison.
- The level of expansion/contraction of the ME in the day- and night-side hemispheres is correlated, in both hemispheres; the day-side and night-side ME expands and contracts in unison as well.
- The GFP is observed to expand/contract from its reference contour in conjunction with the ME; stretching of the magnetic field lines in the middle magnetosphere is likely the dominant effect in determining the expansion of the ME.
- A compressed magnetosphere gives rise to a contracted day-side ME.

In all, these results can be combined to support the following statement:

> The variations in the processes that give rise to the Jovian UV ME and its position in the ionosphere occur globally in Jupiter's magnetosphere, such that the degree of expansion of the ME shows considerable north-south and day-night correlation. These variations occur, to some extent, in response to the variable state of compression of the magnetosphere, which is conveyed to the ME predominantly via a deformation of the magnetic field.

These results greatly improve our ability to use the appearance of the aurora as a proxy for the state of the magnetosphere, which may be retroactively applied to the immense existing corpus of images of Jupiter's UV aurora, as well as providing new image-analysis techniques that will serve as an excellent starting point for the investigation of other arc-like structures in the Jovian aurora.

Acknowledgments

The author is grateful to NASA and contributing institutions which have made the Juno mission possible. This work was funded by NASA's New Frontiers Program for Juno via contract with the Southwest Research Institute. This publication benefits from the support of the Communauté française de Belgique in the context of the FRIA Doctoral Grant awarded to L. A. Head. The author is also grateful to D. Grodent, B. Bonfond, A. Moirano, G. Sicorello, B. Benmahi, V. Hue, J.-C. Gérard, M. Vogt, G. R. Gladstone, and Z. Yao for their assistance in this work.

Further Information

Author's ORCID identifier

0009-0008-1768-7597 (Linus HEAD)

Conflicts of interest

The author declares that there is no conflict of interest.

References

Bagenal, F. and Delamere, P. A. (2011) Flow of mass and energy in the magnetospheres of Jupiter and Saturn. *Journal of Geophysical Research: Space Physics*, **116**(A5). https://doi.org/10.1029/2010JA016294.

Bonfond, B., Grodent, D., Gérard, J.-C., Stallard, T., Clarke, J. T., Yoneda, M., Radioti, A., and Gustin, J. (2012) Auroral evidence of Io's control over the magnetosphere of Jupiter. *Geophysical Research Letters*, **39**(1), L01105. https://doi.org/10.1029/2011GL050253.

Bonfond, B., Gustin, J., Gérard, J.-C., Grodent, D., Radioti, A., Palmaerts, B., Badman, S. V., Khurana, K. K., and Tao, C. (2015) The far-ultraviolet main auroral emission at jupiter – Part 1: Dawn-dusk brightness asymmetries. *Annales Geophysicae*, **33**(10), 1203–1209. https://doi.org/10.5194/angeo-33-1203-2015.

Bonfond, B., Hess, S., Gérard, J.-C., Grodent, D., Radioti, A., Chantry, V., Saur, J., Jacobsen, S., and Clarke, J. T. (2013) Evolution of the Io footprint brightness I: Far-UV observations. *Planetary and Space Science*, **88**, 64–75. https://doi.org/10.1016/j.pss.2013.05.023.

Bonfond, B., Saur, J., Grodent, D., Badman, S. V., Bisikalo, D., Shematovich, V., Gérard, J.-C., and Radioti, A. (2017) The tails of the satellite auroral footprints at Jupiter. *Journal of Geophysical Research: Space Physics*, **122**(8), 7985–7996. https://doi.org/10.1002/2017JA024370.

Chané, E., Saur, J., Keppens, R., and Poedts, S. (2017) How is the Jovian main auroral emission affected by the solar wind? *Journal of Geophysical Research: Space Physics*, **122**(2), 1960–1978. https://doi.org/10.1002/2016JA023318.

Clarke, J. T., Grodent, D., Cowley, S. W. H., Bunce, E. J., Zarka, P., Connerney, J. E. P., and Satoh, T. (2004) Jupiter's aurora. In *Jupiter: The Planet, Satellites and Magnetosphere*, edited by Bagenal, F., Dowling, T. E., and McKinnon, W. B., *Cambridge Planetary Science*, volume 1, chapter 26, pages 639–670. Cambridge University Press, Cambridge (UK).

Connerney, J. E. P., Timmins, S., Herceg, M., and Joergensen, J. L. (2020) A Jovian magnetodisc model for the Juno era. *Journal of Geophysical Research: Space Physics*, **125**(10), e2020JA028138. https://doi.org/10.1029/2020JA028138.

Cowley, S. W. H. and Bunce, E. J. (2001) Origin of the main auroral oval in Jupiter's coupled magnetosphere–ionosphere system. *Planetary and Space Science*, **49**(10-11), 1067–1088. https://doi.org/10.1016/S0032-0633(00)00167-7.

Delamere, P. A., Wilson, R. J., Wing, S., Smith, A. R., Mino, B., Spitler, C., Damiano, P., Sorathia, K., Sciola, A., Caggiano, J., Johnson, J. R., Ma, X., Bagenal, F., Zhang, B., Allegrini, F., Ebert, R., Clark, G., and Brambles, O. (2024) Signatures of open magnetic flux in Jupiter's dawnside magnetotail. *AGU Advances*, **5**(2), e2023AV001111. https://doi.org/10.1029/2023AV001111.

Dumont, M., Grodent, D., Radioti, A., Bonfond, B., Roussos, E., and Paranicas, C. (2018) Evolution of the auroral signatures of Jupiter's magnetospheric injections. *Journal of Geophysical Research: Space Physics*, **123**(10), 8489–8501. https://doi.org/10.1029/2018JA025708.

Feldstein, Y. I. (1986) A quarter of a century with the auroral oval. *Eos, Transactions American Geophysical Union*, **67**(40), 761–767. https://doi.org/10.1029/EO067i040p00761-02.

Gérard, J.-C., Hubert, B., Shematovich, V. I., Bisikalo, D. V., and Gladstone, G. R. (2008) The Venus ultraviolet oxygen dayglow and aurora: Model comparison with observations. *Planetary and Space Science*, **56**(3-4), 542–552. https://doi.org/10.1016/j.pss.2007.11.008.

Grodent, D., Clarke, J. T., Kim, J., Waite, J. H., and Cowley, S. W. H. (2003) Jupiter's main auroral oval observed with HST-STIS. *Journal of Geophysical Research*, **108**(A11), 1389. https://doi.org/10.1029/2003JA009921.

Groulard, A., Bonfond, B., Grodent, D., Gérard, J.-C., Greathouse, T. K., Hue, V., Gladstone, G. R., and Versteeg, M. H. (2024) Dawn–dusk asymmetry in the main auroral emissions at Jupiter observed with Juno-UVS. *Icarus*, **413**, 116 005. https://doi.org/10.1016/j.icarus.2024.116005.

Khurana, K. K. (2001) Influence of solar wind on Jupiter's magnetosphere deduced from currents in the equatorial plane. *Journal of Geophysical Research: Space Physics*, **106**(A11), 25 999–26 016. https://doi.org/10.1029/2000JA000352.

Khurana, K. K., Kivelson, M. G., Vasyliunas, V. M., Krupp, N., Woch, J., Lagg, A., Mauk, B. H., and Kurth, W. S. (2004) The configuration of Jupiter's magnetosphere. In *Jupiter: The Planet, Satellites and Magnetosphere*, edited by Bagenal, F., Dowling, T. E., and McKinnon, W. B., *Cambridge Planetary Science*, volume 1, chapter 24, pages 593–616. Cambridge University Press, Cambridge (UK).

Nichols, J. D. (2011) Magnetosphere-ionosphere coupling in Jupiter's middle magnetosphere: Computations including a self-consistent current sheet magnetic field model. *Journal of Geophysical Research: Space Physics*, **116**(A10), A10232. https://doi.org/10.1029/2011JA016922.

Nichols, J. D., Badman, S. V., Bagenal, F., Bolton, S. J., Bonfond, B., Bunce, E. J., Clarke, J. T., Connerney, J. E. P., Cowley, S. W. H., Ebert, R. W., Fujimoto, M., Gérard, J.-C., Gladstone,

G. R., Grodent, D., Kimura, T., Kurth, W. S., Mauk, B. H., Murakami, G., McComas, D. J., Orton, G. S., Radioti, A., Stallard, T. S., Tao, C., Valek, P. W., Wilson, R. J., Yamazaki, A., and Yoshikawa, I. (2017) Response of Jupiter's auroras to conditions in the interplanetary medium as measured by the Hubble Space Telescope and Juno. *Geophysical Research Letters*, **44**(15), 7643–7652. https://doi.org/10.1002/2017GL073029.

Nichols, J. D., Clarke, J. T., Gérard, J. C., and Grodent, D. (2009) Observations of Jovian polar auroral filaments. *Geophysical Research Letters*, **36**(8), L08 101. https://doi.org/10.1029/2009GL037578.

Palmaerts, B., Grodent, D., Bonfond, B., Yao, Z. H., Guo, R. L., Gérard, J.-C., Haewsantati, K., Gladstone, G. R., Greathouse, T. K., Hue, V., and Nichols, J. D. (2023) Overview of a large observing campaign of Jupiter's aurora with the Hubble Space Telescope combined with Juno-UVS data. *Icarus*, **408**, 115815. https://doi.org/10.1016/j.icarus.2023.115815.

Potter, N. (2021) Revealed: Jupiter's secret power source. IEEE Spectrum. https://spectrum.ieee.org/jupiter-auroras-jaxa-nasa.

Promfu, T., Nichols, J. D., Wannawichian, S., Clarke, J. T., Vogt, M. F., and Bonfond, B. (2022) Ganymede's auroral footprint latitude: Comparison with magnetodisc model. *Journal of Geophysical Research: Space Physics*, **127**(12), e2022JA030712. https://doi.org/10.1029/2022JA030712.

Roth, L., Boissier, J., Moullet, A., Sánchez-Monge, Á., de Kleer, K., Yoneda, M., Hikida, R., Kita, H., Tsuchiya, F., Blöcker, A., Gladstone, G. R., Grodent, D., Ivchenko, N., Lellouch, E., Retherford, K. D., Saur, J., Schilke, P., Strobel, D., and Thorwirth, S. (2020) An attempt to detect transient changes in Io's SO_2 and NaCl atmosphere. *Icarus*, **350**, 113925. https://doi.org/10.1016/j.icarus.2020.113925.

Saur, J. (2004) A model of Io's local electric field for a combined Alfvénic and unipolar inductor far-field coupling. *Journal of Geophysical Research: Space Physics*, **109**(A1), A01210. https://doi.org/10.1029/2002JA009354.

Saur, J., Neubauer, F. M., Connerney, J. E. P., Zarka, P., and Kivelson, M. G. (2004) Plasma interaction of Io with its plasma torus. In *Jupiter: The Planet, Satellites and Magnetosphere*, edited by Bagenal, F., Dowling, T. E., and McKinnon, W. B., *Cambridge Planetary Science*, volume 1, chapter 22, pages 537–560. Cambridge University Press, Cambridge (UK).

Soret, L., Gérard, J.-C., Schneider, N., Jain, S., Milby, Z., Ritter, B., Hubert, B., and Weber, T. (2021) Discrete aurora on Mars: Spectral properties, vertical profiles, and electron energies. *Journal of Geophysical Research: Space Physics*, **126**(10), e2021JA029495. https://doi.org/10.1029/2021JA029495.

Tao, C., Kimura, T., Tsuchiya, F., Muirakami, G., Yoshioka, K., Yamazaki, A., Badman, S. V., Misawa, H., Kita, H., Kasaba, Y., Yoshikawa, I., and Fujimoto, M. (2018) Variation of Jupiter's aurora observed by Hisaki/EXCEED: 3. Volcanic control of Jupiter's aurora. *Geophysical Research Letters*, **45**(1), 71–79. https://doi.org/10.1002/2017GL075814.

Vogt, M. F., Bagenal, F., and Bolton, S. J. (2022a) Magnetic field conditions upstream of Ganymede. *Journal of Geophysical Research: Space Physics*, **127**(12), e2022JA030497. https://doi.org/10.1029/2022JA030497.

Vogt, M. F., Kivelson, M. G., Khurana, K. K., Walker, R. J., Bonfond, B., Grodent, D., and Radioti, A. (2011) Improved mapping of Jupiter's auroral features to magnetospheric sources. *Journal of Geophysical Research: Space Physics*, **116**(A3), A03220. https://doi.org/10.1029/2010JA016148.

Vogt, M. F., Rutala, M., Bonfond, B., Clarke, J. T., Moore, L., and Nichols, J. D. (2022b) Variability of Jupiter's main auroral emission and satellite footprints observed with HST during the Galileo Era. *Journal of Geophysical Research: Space Physics*, **127**(2), e2021JA030011. https://doi.org/10.1029/2021JA030011.

Yao, Z. H., Bonfond, B., Grodent, D., Chané, E., Dunn, W. R., Kurth, W. S., Connerney, J. E. P., Nichols, J. D., Palmaerts, B., Guo, R. L., Hospodarsky, G. B., Mauk, B. H., Kimura, T., and Bolton, S. J. (2022) On the relation between auroral morphologies and compression conditions of Jupiter's magnetopause: Observations from Juno and the Hubble Space Telescope. *Journal of Geophysical Research: Space Physics*, **127**(10), e2021JA029894. https://doi.org/10.1029/2021JA029894.